DOI: 10.1534/genetics.107.084079

Barren inflorescence1 Functions in Organogenesis During Vegetative and Inflorescence Development in Maize

Solmaz Barazesh and Paula McSteen[1]

Department of Biology, Pennsylvania State University, University Park, Pennsylvania 16802

Manuscript received November 5, 2007
Accepted for publication February 15, 2008

ABSTRACT

Maize (*Zea mays*) has a highly branched inflorescence due to the production of different types of axillary meristems. Characterization of the *barren inflorescence* class of mutants has led to the discovery of genes required for axillary meristem initiation in the inflorescence. Previous studies showed that *barren inflorescence2* (*bif2*) encodes a serine/threonine protein kinase that regulates auxin transport, and *barren stalk1* (*ba1*) encodes a basic helix-loop-helix transcription factor that acts downstream of auxin transport. Here, we characterize *Barren inflorescence1* (*Bif1*), a classical semidominant mutation of maize. Developmental, histological, and genetic analyses show that *Bif1* mutants are defective in the initiation of all axillary meristems in the inflorescence. Real time RT–PCR experiments show that both *bif2* and *ba1* are expressed at lower levels in *Bif1* mutants. Double-mutant analyses demonstrate that *Bif1* exhibits an epistatic interaction with *ba1* and a synergistic interaction with *bif2*. The dramatic phenotypic enhancement observed in *Bif1; bif2* double mutants implies that *bif1* plays an overlapping role with *bif2* in the initiation of lateral organs during vegetative development. The phenotypic resemblance of *Bif1* to *bif2* mutants and the reduction of auxin transport in *Bif1* mutants suggest that *bif1* functions as a regulator of auxin transport in maize.

ORGANOGENESIS in plants is controlled by meristems (Steeves and Sussex 1989). The peripheral zone of the meristem initiates organ primordia while the central zone remains undifferentiated to allow organogenesis to continue indefinitely (McSteen and Hake 1998; Veit 2006). Auxin plays a fundamental role in organogenesis in the peripheral zone of the meristem (Reinhardt *et al.* 2000, 2003; Vernoux *et al.* 2000). Plants with mutations in genes required for auxin biosynthesis, transport, or response have defects in organogenesis (Okada *et al.* 1991; Bennett *et al.* 1995; Przemeck *et al.* 1996; Vernoux *et al.* 2000; Cheng *et al.* 2006, 2007). These and other studies have shown that auxin is required for leaf initiation during vegetative development and flower initiation during reproductive development (Okada *et al.* 1991; Reinhardt *et al.* 2000, 2003; Benkova *et al.* 2003; Scanlon 2003; Heisler *et al.* 2005; Cheng and Zhao 2007; Wu and McSteen 2007).

During the vegetative phase of growth, the shoot apical meristem (SAM) at the tip of the developing shoot reiteratively produces phytomers, consisting of node, internode, leaf, and axillary meristem located in the axil of the leaf (Steeves and Sussex 1989; McSteen and Leyser 2005). Axillary meristems can grow out to become a lateral branch, known as a tiller in maize, which reiterates the growth of the main shoot. During the reproductive phase of growth, the shoot apical meristem converts to an inflorescence meristem that produces modified phytomers. In many plants, the leaves are reduced to form bract leaves and the axillary meristems are enlarged to produce the flowers (Steeves and Sussex 1989). In maize, highly branched inflorescences are produced (McSteen *et al.* 2000; Bommert *et al.* 2005; Bortiri and Hake 2007). The male inflorescence, the tassel, grows at the apex of the plant and is composed of a main spike with several long branches at the base (Figure 1A). The main spike and branches produce short branches called spikelet pairs. The spikelet is the building block of all grass inflorescences (Clifford 1987; Kellogg 2000). In maize, the spikelet is composed of two leaf-like glumes enclosing two florets. The female inflorescence, the ear, is produced from an axillary meristem located several nodes below the tassel. In both tassel and ear, the florets are enclosed by leaf-like structures called lemma and palea surrounding a pair of petal-like structures, called lodicules, and the reproductive organs, the stamens and carpels. The carpels abort in the tassel and the stamens abort in the ear to produce separate male and female inflorescences (Irish 1996).

To produce this highly branched inflorescence, the inflorescence meristem produces four types of axillary meristems (Table 1), which give rise to the various

[1]*Corresponding author:* 208 Mueller Lab, Department of Biology, Pennsylvania State University, University Park, PA 16802.
E-mail: pcm11@psu.edu

TABLE 1

Axillary meristems in the maize inflorescence

Order	Meristem	Product	Determinacy
1°	Branch (BM)	Branches	Indeterminate
1°	Spikelet pair (SPM)	Spikelet pairs	Determinate
2°	Spikelet (SM)	Florets	Determinate
3°	Floral (FM)	Floral organs	Determinate

structures of the mature inflorescence (Cheng *et al.* 1983; Irish 1997; McSteen *et al.* 2000; Bommert *et al.* 2005). The primary axillary meristems have two alternative fates. The first primary axillary meristems that arise are the branch meristems (BMs). BMs are indeterminate and grow out to become long branches at the base of the tassel, which reiterate the growth of the main spike (Table 1). The next primary axillary meristems that arise are the spikelet pair meristems (SPMs). SPMs are determinate and give rise to short branches bearing a pair of spikelets (Table 1). The SPMs produce the secondary axillary meristems called spikelet meristems (SMs), which then produce the tertiary axillary meristems called floral meristems (FMs), which finally produce the floral organs. The fate of the primary axillary meristems as indeterminate (branch) *vs.* determinate (spikelet pair) is regulated by the *ramosa* (*ra*) pathway (Vollbrecht *et al.* 2005; Bortiri *et al.* 2006a; McSteen 2006; Satoh-Nagasawa *et al.* 2006; Kellogg 2007). The *ra1* and *ra2* genes encode transcription factors that are required to impose determinacy on the SPM (Vollbrecht *et al.* 2005; Bortiri *et al.* 2006a). In the *ra1* mutant, there are additional long branches in the tassel and the ear (Gernart 1912; Vollbrecht *et al.* 2005).

The *barren inflorescence* loci in maize identify genes required for axillary meristem initiation. *barren stalk1* (*ba1*) encodes a basic helix-loop-helix transcription factor required for axillary meristem initiation during both vegetative and reproductive development (Gallavotti *et al.* 2004). *ba1* mutants do not produce tillers, ears, branches, spikelets, and florets (Ritter *et al.* 2002). *barren inflorescence2* (*bif2*) mutants also have fewer ears and fewer branches, spikelets, florets, and floral organs due to defects in the initiation of axillary meristems in the inflorescence (McSteen and Hake 2001). *bif2* mutants also have defects in axillary meristem initiation during vegetative development (McSteen *et al.* 2007). The *bif2* gene encodes a serine/threonine protein kinase co-orthologous to *PINOID*, which regulates auxin transport in Arabidopsis (Christensen *et al.* 2000; Benjamins *et al.* 2001; Lee and Cho 2006; McSteen *et al.* 2007).

Here, we characterize another *barren inflorescence* mutation, *Barren inflorescence1* (*Bif1*). *Bif1* is a semidominant mutation that confers the phenotype of fewer branches, spikelets, florets, and floral organs in the inflorescence. Although *Bif1* is a classical mutation of maize first isolated >30 years ago (Neuffer *et al.* 1997), the phenotype has not previously been analyzed in detail. Here, we report that the defects in *Bif1* mutants are due to defects in the initiation of axillary meristems in the inflorescence. We tested the interaction between *Bif1* and *bif2* or *ba1*, using expression and double-mutant analyses. We show that *Bif1* is epistatic to *ba1* and that *ba1* expression is greatly reduced in *Bif1* mutants. We show that *Bif1* mutants share many phenotypic similarities with *bif2* mutants and that *bif2* expression is also reduced in *Bif1* mutants. The dramatic enhancement of phenotype seen in *Bif1; bif2* double-mutant plants indicates that *bif1* plays a redundant role with *bif2* in the initiation of leaves during vegetative development. *Bif1* mutants have reduced levels of auxin transport, implying that the function of *bif1* is in the regulation of auxin transport.

MATERIALS AND METHODS

Analysis of the mature inflorescence phenotype of *Bif1*: The *Bif1-1440* allele was obtained from the Maize Genetics Coop Stock Center (stock no. 827C) and backcrossed eight times into the B73 genetic background. Quantitative analysis was performed on plants grown until maturity (9–10 weeks) in the field during the summer in Rock Springs, Pennsylvania. Data representative of one field season are presented. For analysis of branch and spikelet number, 8–10 plants of each genetic class were analyzed. For floret and floral organ number, 100 spikelets of each genetic class were analyzed.

Double-mutant analyses: All mutant stocks were backcrossed a minimum of five times to B73 before being used to generate double mutants with *Bif1*. All double-mutant families were grown in the field during the summer in Rock Springs, Pennsylvania. To reduce environmental effects, all families were planted twice in different field locations and in two separate field seasons. Two to three F_2 families of 120 kernels were planted in each location. Data presented here are a representative subset of the data collected during the 2007 field season. Chi-square analysis failed to reject the null hypothesis for the expected number of plants in each genotypic class (supplemental Table S1).

Bif1; ra1: The *ra1-R* allele was used to generate *Bif1; ra1* double-mutant segregating families (Vollbrecht *et al.* 2005). At maturity *Bif1; ra1* double mutants were scored by tassel and ear phenotype. Inflorescence architecture of at least 10 plants of each genetic class was analyzed. The number of primary and secondary tassel branches and the total number of spikelets were counted. The spikelet number per branch at the base of the tassel was also counted, as well as the number of spikelets in the top two centimeters of the main spike.

Bif1; bif2: Families segregating *Bif1; bif2* double mutants were generated using the *bif2-77* allele (McSteen *et al.* 2007). For genotyping, leaf tissue was collected from 2-week-old plants into 96-well plates and ground using a Tissue Lyzer (QIAGEN, Valencia, CA). DNA was extracted according to a protocol modified for 96-well plate format from Chen and Dellaporta (1994) with the phenol chloroform extraction step omitted. PCR was carried out to genotype the plants for the *bif2-77* mutation, using primers bif2-57 (5′ CAG CCT GCC GCG CTG CTC CAGC 3′) and bif2-250 (5′ CGG CGC AGC AGC CTG AAG TCC 3′), which are designed to cross the site of

the insertion in this *bif2* allele (McSteen *et al.* 2007). A second set of PCR reactions, using primer bif2-57 with a primer located in the insertion (bif2-77, 5′ CAG TGG CGG GCC TAG AAA TTT G 3′), was used to confirm this result. *Bif1/Bif1; bif2/bif2* plants were easily identified as plants genotyped as homozygous for the *bif2* mutation but that also had extremely short stature and a severe tassel phenotype. Initial phenotype analysis revealed an excess of plants with a *Bif1/Bif1* homozygous phenotype. This excess was attributed to *Bif1/+; bif2/bif2* double mutants that resembled severe *Bif1* homozygotes in phenotype but were genotyped as homozygous for the *bif2* mutation. Further confirmation of this result was obtained by crossing *Bif1/+; bif2/+* plants to *+/+; bif2/+* plants and determining that one-eighth of the progeny resembled *Bif1* homozygotes.

At maturity, plant height was measured on every plant from the ground to the tip of the tassel. To count leaf number, every fifth leaf of each plant was clipped with pinking shears, beginning at 3 weeks after emergence and at regular intervals throughout the field season. This enabled us to obtain an accurate measure of total leaf number at the end of the field season because if we had counted only at the end of the field season, we would have missed the leaves that had senesced. Ten plants of each genetic class were used for analysis of tassel branch number and spikelet number.

Bif1; ba1: The *ba1-ref* allele was used to generate *Bif1; ba1* double-mutant segregating families (Gallavotti *et al.* 2004). Tissue was collected and DNA extracted as described for the *Bif1; bif2* plants. Plants were genotyped using primer ba04 (5′ TGG CAT TGC ATG GAA GCG TGT ATG AGC 3′) located in the *ba1* promoter and primer ba05 (5′ TCC TAG ACA TGC ATA TCT GAA CCA GAG CT 3′) located in the helitron in the *ba1-ref* allele, which amplified a product in *ba1* heterozygous and homozygous plants. A second PCR reaction with primers ba04 and ba07 (5′ GCT AAG CTA CTG TAA GCG GGA TGG ACA 3′) amplified a product in wild-type and heterozygous plants. *Bif1/Bif1; ba1/ba1* double mutants were classified as plants genotyped as homozygous for *ba1*, but with a smooth, thin tassel rachis similar to *Bif1* homozygotes. *Bif1/+; ba1/ba1* double mutants were classified as plants genotyped as homozygous for *ba1*, which looked like *ba1* but with a slightly smoother tassel rachis.

Statistical analysis: The computer program Minitab v.15 (Minitab, State College, PA) was used to perform all statistical analysis. Data sets were compared with two-sample two-tailed *t*-tests. Data presented in bar charts are the mean value of the data, and all error bars show standard error of the mean.

Scanning electron microscopy, RNA *in situ* hybridization, and histology: Tassels were obtained from families segregating for *Bif1* grown in the greenhouse for 5 weeks. The tassels were dissected and fixed on ice overnight in 3.7% formalin, 50% ethanol, 10% acetic acid (FAA) and then dehydrated through an ethanol series. Ears were obtained from *Bif1* plants grown in the field for 8 weeks. Ears were dissected and fixed on ice overnight in 4% formaldehyde in phosphate-buffered saline. For scanning electron microscopy (SEM), meristems were critical-point dried (BAL-TEC CPD 030; Techno Trade, Manchester, NH) and then mounted onto carbon stubs. The samples were sputter coated with a 0.7-Å layer of gold palladium (BAL-TEC SCD 050, Techno Trade) and viewed by SEM (JSM 5400; JEOL, Peabody, MA), using a 10-kV accelerating voltage. For sectioning, samples were embedded in paraffin wax (Paraplast Plus; McCormick Scientific, St. Louis). Sections 8 μm thick were cut using a Finnesse paraffin microtome (Thermo Fisher, Waltham, MA) and mounted onto coated slides (Probe-On Plus; Fisher Scientific, Waltham, MA). For RNA *in situ* hybridization, the slides were probed with a DIG-labeled RNA antisense probe of *kn1* according to Jackson *et al.* (1994). For histology, the slides were dewaxed using histoclear (National Diagnostics, Atlanta), hydrated through an ethanol series, stained in 0.05% Toluidine Blue O (TBO) for 30 sec, dehydrated, and mounted with a coverslip using Histomount (Thermo-Shandon, Pittsburgh). All slides were viewed under bright field with an Eclipse 80i upright microscope (Nikon, Melville, NY) and photographed with a DXM1200F digital camera (Nikon).

Expression analysis: Total RNA was isolated from 5- to 6-week-old tassels (5–7 mm) and 8-week-old ears (20–22 mm) from *Bif1* homozygotes and normal siblings, using the Nucleospin RNA plant kit following the manufacturer's protocol (Macherey-Nagel, Durel, Germany). One tassel or ear (~8–12 mg fresh weight) was used per RNA extraction, with three biological replicates of each sample type. A total of 200 ng of RNA from each sample were DNase treated, using the DNase I kit (Ambion, Austin, TX) to remove genomic DNA contamination. Reverse transcription was carried out using the ABI High-Capacity RT kit (Applied Biosystems, Foster City, CA), with incubation at 25° for 10 min and then 37° for 2 hr. Real-time RT–PCR primers and 5′ FAM- (Carboxyfluorescein) and 3′ BHQ1- (Black Hole Quencher) labeled Taqman probes (Biosearch Technologies, Novato, CA) were designed, using Primer Express version 2.0 software (Applied Biosystems). Five microliters of cDNA were used as template for real-time RT–PCR reactions using TaqMan 2X Universal mix (Applied Biosystems), except that Betaine (Sigma, St Louis) was added to a final concentration of 0.5 m in the *bif2* reactions. RT–PCR reactions were carried out in 96-well plates using an ABI 7300 real-time PCR machine (Applied Biosytems). For detection of *bif2* expression, the Taqman probe was (FAM-5′ CTC CGC CAC CGC ATG CCC 3′-BHQ) and the RT–PCR primers were bif2F (5′ CTG CGT CGT CAC GGA GTT C 3′) and bif2R (5′ TGC CCA TCA TGT GCA GGT ACT 3′). For detection of *ba1* expression, the Taqman probe was (FAM-5′ ACG CGG CTT CCC CAT CAT CCA 3′-BHQ) and the RT–PCR primers were ba1F (5′ TGG ATC CAT ATC ACT ACC AAA CCA 3′) and ba1R (5′ ACC GGG TGC TGG AGG TAA G 3′). The control for normalization was *ubiquitin*: the Taqman probe was (5′ FAM-AAA TCC ACC CGT CGG CAC CTC C 3′-BHQ) and RT–PCR primers were ubqF (5′ CTC TTT CCC CAA CCT CGT GTT 3′) and ubqR (5′ ACG AGC GGC GTA CCT TGA 3′). Three technical replicates of each real-time PCR reaction were performed on three biological replicates for each experiment and the entire experiment was repeated twice. Normalized relative expression levels were determined using the comparative threshold method (Livak and Schmittgen 2001).

Auxin transport assays: Auxin transport assays were performed using a method modified from Okada *et al.* (1991) and McSteen *et al.* (2007). Immature ear inflorescences were dissected from plants grown in the field for 8 weeks. The immature ears ranged from 2 to 3 cm in size. At this stage of development, the inflorescence meristem was still initiating SPMs at the tip and floral organs were being produced at the base. Two centimeters of the tip of the ear was placed in either orientation into 2-ml tubes containing 100 μl 1.5 μm 3-[5(n)-^{3}H] indole acetic acid (specific activity 25 Ci/mmol; GE Healthcare, Piscataway, NJ) in 0.5× Murashige and Skoog medium (Sigma, St. Louis). Some tubes also contained 20 μm *N*-1-naphthylphthalamic acid (Chemservice, West Chester, PA). After 24 hr incubation in the dark, the immature ear pieces were blotted and 5 mm from the end that was not immersed in solution was placed in scintillation fluid (Ready safe; Beckman Coulter, Fullerton, CA) and counted in a liquid scintillation counter (LSC6000, Beckman Coulter). For the initial experiment on normal ears, three ears were used for each treatment and the experiment was repeated three times. For the experiment on *Bif1* mutants, three ears from each genotypic class were used and the experiment was repeated

four times. Data that are representative of one experiment are presented.

RESULTS

The *Bif1* mutation was recovered from an EMS mutagenesis experiment (Neuffer and Sheridan 1977) and was mapped to chromosome 8 using genetic and cytogenetic tools (http://www.maizegdb.org). Using SSR markers, we fine mapped *Bif1* to between *idp98* and *umc1360* in bin 8.02. *Bif1* is a semidominant mutation with the homozygote having a more severe phenotype than the heterozygote. The *Bif1* mutation confers the phenotype of fewer branches and spikelets in the tassel and fewer kernels in the ear but the phenotype had not previously been analyzed in detail (Coe *et al.* 1988; Sheridan 1988; Veit *et al.* 1993; Neuffer *et al.* 1997; McSteen *et al.* 2000).

***Bif1* mutants produce fewer branches and spikelets:** *Bif1* mutant tassels had a sparse appearance with fewer branches and spikelets compared to normal siblings (Figure 1A). The tassels of plants that were homozygous for *Bif1* were more strongly affected than heterozygotes (Figure 1A). Plants heterozygous for *Bif1* produced ears with irregular rowing due to the reduced number of kernels and the tip was barren (Figure 1B). Plants homozygous for *Bif1* produced ears with very few kernels, such that bare rachis was visible (Figure 1B).

Quantitative analysis of the mature *Bif1* tassel showed that *Bif1* mutants fail to produce the full complement of tassel branches (Figure 1C). Analysis of spikelet number showed a statistically significant reduction in spikelet number in plants heterozygous and homozygous for *Bif1* (Figure 1D). In plants homozygous for *Bif1*, spikelets that formed were sometimes produced singly instead of in pairs (Figure 1E). The reduced number of branches and spikelets produced suggests that the initiation or maintenance of primary axillary meristems, the BM and SPM, is defective in *Bif1* inflorescences.

***Bif1* mutants fail to initiate SPMs:** The phenotype of the mature *Bif1* inflorescence suggested that there were defects in the early stages of inflorescence development. To test this, SEM was used to visualize the developing inflorescence. By 5 weeks of growth, normal inflorescences had initiated several lateral branches, with SPMs visible as regular bumps on the flanks of both the main spike and the branches (Figure 2A). At the same stage of development, plants heterozygous for *Bif1* had a reduced number of SPMs (Figure 2B). Plants homozygous for *Bif1* had a more severe phenotype with very few or, in some cases, no SPMs (Figure 2C). The barren surface of the rachis was very slightly ridged (Figure 2C). The *Bif1* homozygous ear had a similar phenotype as the tassel with few SPMs initiated (Figure 2E). Unlike the tassel, the ear inflorescence meristem was fasciated (Figure 2E).

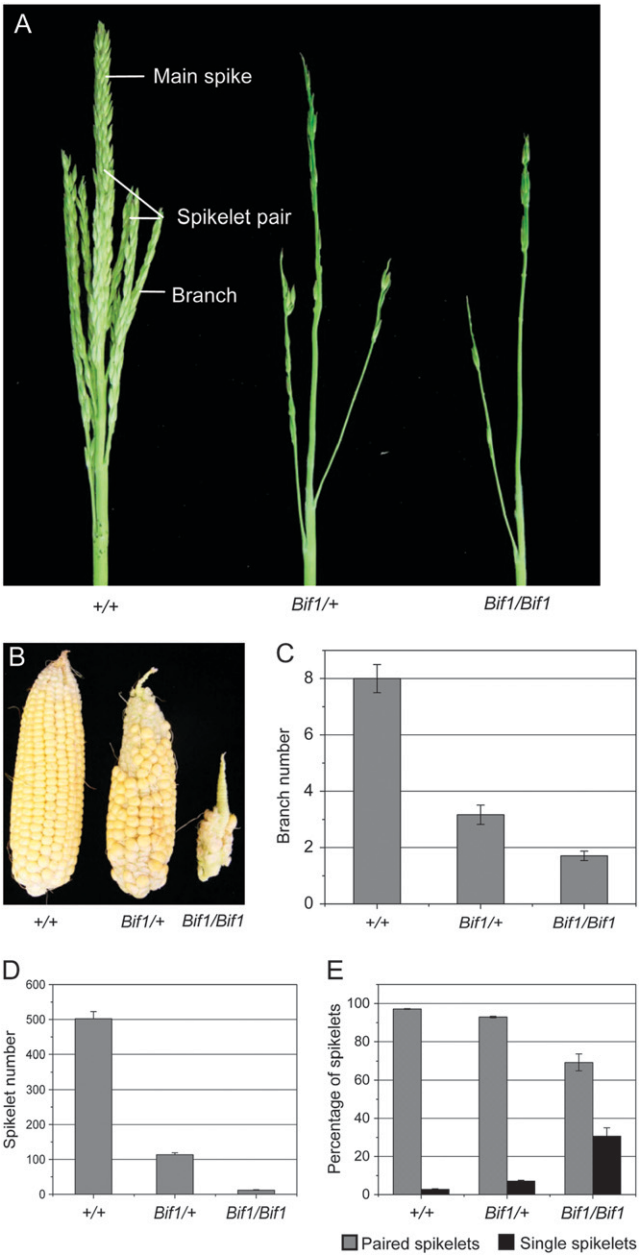

Figure 1.—Mature inflorescence phenotype of the *Bif1* mutant. (A) Mature tassels of normal, *Bif1*/+, and *Bif1/Bif1* plants. In the normal tassel, long branches are indicated at the base of the main spike. Spikelet pairs cover the branches and the main spike. In the *Bif1* mutants, there are reduced numbers of branches and spikelets in the tassel. (B) Mature ears of normal, *Bif1*/+, and *Bif1/Bif1* plants, showing fewer kernels and disorganized rows in *Bif1* mutants. (C) Quantification of tassel branch number. (D) Quantification of tassel spikelet number. (E) Percentage of spikelets that occur singly *vs.* paired. Bars represent mean value and error bars represent standard error of the mean.

To determine if there was any histological evidence of SPM formation, we used TBO to stain sections of developing *Bif1* inflorescences. As meristematic cells have smaller vacuoles than differentiated cells, SPMs stain more intensely with TBO than surrounding tissue. In

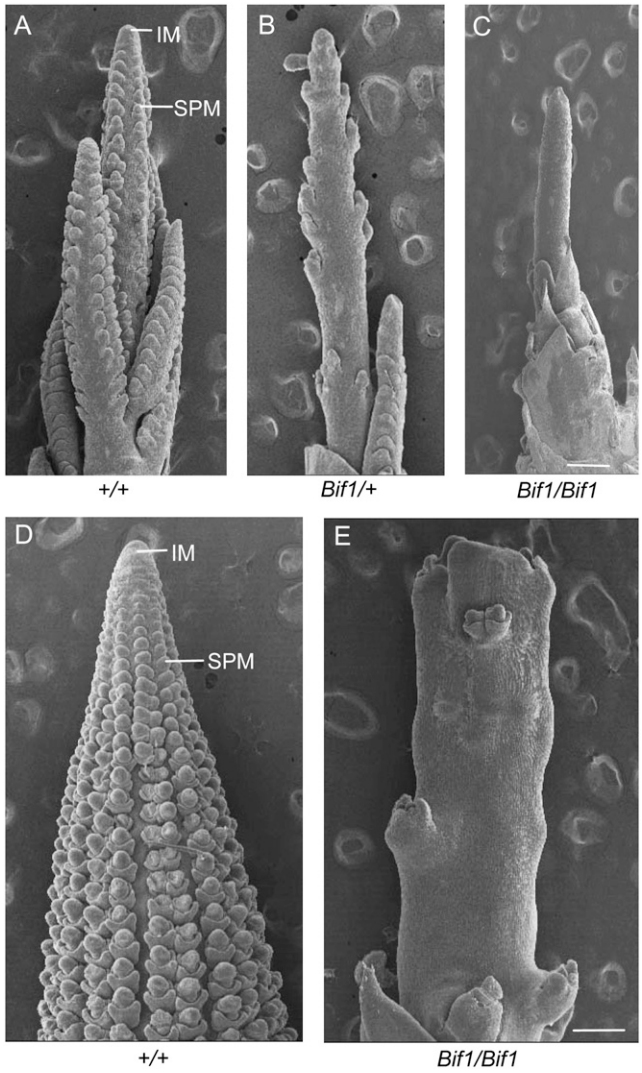

FIGURE 2.—Scanning electron microscopy (SEM) images of developing *Bif1* inflorescences. (A) Normal tassel, showing files of developing spikelet pair meristems (SPMs) on the flanks of the inflorescence meristem (IM). (B) *Bif1/+* tassel, with reduced numbers of SPMs. (C) *Bif1/Bif1* tassel with few SPMs. (D) Normal ear, showing organized rows of SPMs. (E) *Bif1/Bif1* ear, with a fasciated inflorescence meristem and few SPMs. Bar, 100 μm.

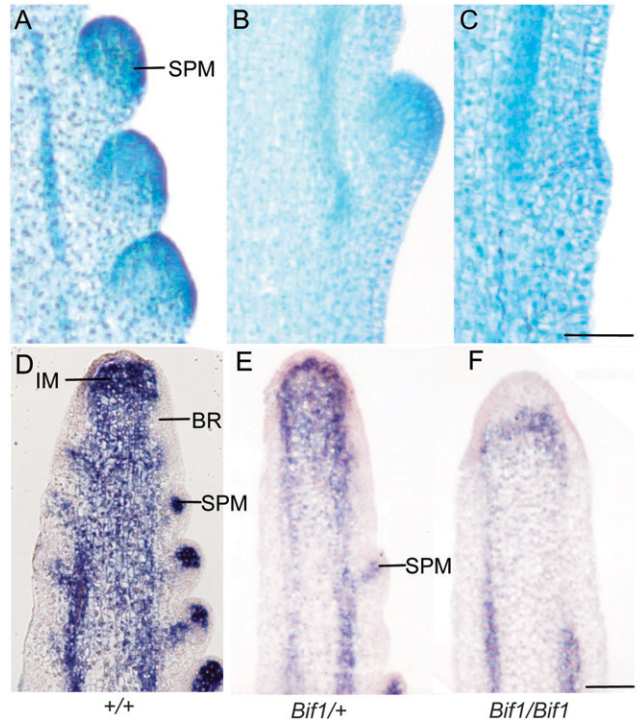

FIGURE 3.—Histology and RNA *in situ* hybridization with *kn1* in developing *Bif1* tassels. (A–C) Longitudinal sections of 5-week-old tassels stained with TBO, with SPMs visible as areas of intense staining. (A) Three developing SPMs on the flanks of the inflorescence meristem in a normal tassel. (B) *Bif1/+*, showing a single SPM in the same area as there are three SPMs in normal. (C) *Bif1/Bif1* with a slight protrusion on the surface of the rachis but no evidence of developing SPM. (D–F) RNA *in situ* hybridization with *kn1*. (D) Meristematic cells and vasculature are indicated by *kn1* expression in normal tassels. The absence of *kn1* on the flanks of the inflorescence meristem (IM) indicates the formation of the suppressed bract primordia (BR) that subtend SPMs. (E) *Bif1/+* inflorescences have fewer areas of *kn1* expression on the flanks of the inflorescence. (F) *Bif1/Bif1* inflorescence with *kn1* expression only in the inflorescence meristem and in the vasculature. Bar, 100 μm.

normal inflorescences, developing SPMs were visible as regular groups of densely staining cells on the flanks of the inflorescence (Figure 3A). In *Bif/+* plants, SPMs visible on the flanks of the inflorescence looked similar to normal except there were fewer of them (Figure 3B). *Bif1* homozygotes mostly did not produce SPMs (Figure 3C). Instead, the surface of barren regions of the inflorescence occasionally had very slightly raised protrusions that were less intensely stained than SPMs, indicating that the slight ridges visible by SEM consist of differentiated tissue (Figure 3C).

To determine if there was any molecular evidence of SPM formation, RNA *in situ* hybridization with *kn1* was used as a marker to identify meristematic tissues. *kn1* is expressed in meristems, where it is required for meristem maintenance, and is not expressed as organ primordia differentiate (JACKSON *et al.* 1994; KERSTETTER *et al.* 1997; VOLLBRECHT *et al.* 2000). In normal plants, *kn1* expression was clearly visible in the inflorescence meristem and in the vasculature and stem (Figure 3D). *kn1* was not expressed on the flanks of the inflorescence meristem, as bract primordia (whose subsequent growth is suppressed) initiate (labeled BR in Figure 3D). However, *kn1* was strongly expressed in SPMs that form in the axils of bract primordia (Figure 3D). In *Bif1* mutants, *kn1* was expressed as normal in the inflorescence meristem, vasculature, and stem (Figure 3, E and F). In plants heterozygous for *Bif1*, areas with no *kn1* expression were interspersed with areas of *kn1* expression as expected for the few SPMs that initiate (Figure 3E). In plants homozygous for *Bif1*, there was usually no evidence of SPM formation on the flanks of the

inflorescence meristem (Figure 3F). As downregulation of *kn1* was visible on the flanks of the *Bif1* inflorescence meristem (Figure 3, E and F), this indicates that bract primordia are set aside in *Bif1* mutants and that the occasional small ridges visible in *Bif1* mutants may be suppressed bract primordia. However, the *in situs* with *kn1* clearly show that SPMs do not form in the axils of the bract primordia in plants homozygous for *Bif1*.

***Bif1* mutants have defects in SM initiation rather than in SPM determinacy:** In normal plants, on the main spike and lateral branches, the SPMs produce a pair of SMs. *Bif1* mutants have a reduced number of spikelets, in large part due to the reduced numbers of SPMs. When SPMs initiate in *Bif1* mutants they often produce single instead of paired spikelets (Figure 1E). This indicates that *Bif1* mutants have defects either in SM initiation or in SPM determinacy. To distinguish between these two possibilities, we constructed double mutants between *Bif1* and *ramosa1* (*ra1*). *ra1* encodes an EPF zinc-finger transcription factor that confers determinacy on the SPM (Vollbrecht *et al.* 2005). In *ra1* mutants, SPMs lack determinacy and grow out to become long indeterminate branches instead of producing determinate spikelet pairs (Gernart 1912; Vollbrecht *et al.* 2005). As a result, *ra1* mutants produce additional long branches in both the tassel and the ear (Figure 4, A and B).

We found that even in the *ra1* mutant background, *Bif1* homozygotes were unable to make additional long branches in the tassel (Figure 4A). The *Bif1/Bif1; ra1/ra1* double mutant had a barren tassel phenotype similar to *Bif1* (Figure 4A). Quantitative analysis showed that total branch number and spikelet number were not statistically different between *Bif1/Bif1; ra1/ra1* and *Bif1/Bif1* (branch number, *P*-value = 0.054; spikelet number, *P*-value = 0.192; Figure 4, F and G). Therefore, when no SPMs were produced in *Bif1* homozygotes, *ra1* could not act on them. On the other hand, in the *Bif1/Bif1; ra1/ra1* ear, several branches grew out from the rachis (Figure 4B, close-up shown in Figure 4E). It appeared that when SPMs initiated in the *Bif1/Bif1; ra1/ra1* ear, they converted to branches due to the absence of *ra1* (Figure 4, B and E). Hence, the *Bif1* mutant does not have defects in SPM determinacy once SPMs have initiated.

Further insight was obtained by characterizing *Bif1/+; ra1/ra1* double mutants. The tassel of *Bif1/+; ra1/ra1* double mutants had more long branches and spikelets than *Bif1/+* (Figure 4A). Quantitative analysis showed that there was a significant increase in branch number in *Bif1/+; ra1/ra1* compared to *Bif1/+* (*P*-value <0.001, Figure 4F). This suggests that when SPMs initiated, they grew out to become lateral branches. However, the branches on *Bif1/+; ra1/ra1* were more barren than typical *ra1* branches and did not have a statistically different number of spikelets compared to *Bif1/+* plants (*P*-value = 0.94; Figure 4, G–I). Similarly, the *Bif1/+; ra1/ra1* ear was more highly branched than the *Bif1/Bif1; ra1/ra1* ear but few spikelets were produced on the branches (Figure 4B, close-up of an individual branch shown in Figure 4D). These results indicate that *Bif1* mutants have defects in the initiation of secondary axillary meristems, SMs, rather than defects in the determinacy of primary axillary meristems, SPMs.

Spikelet and floral meristems are defective in *Bif1* mutants: Dissection of the few spikelets produced in *Bif1* mutant plants indicated that *Bif1* spikelets had fewer florets than normal and the florets had fewer floral organs. To quantify these defects, 100 spikelets were dissected from both *Bif1* heterozygous and homozygous plants and the number of florets and floral organs was determined relative to normal sibs.

In normal plants, each spikelet bears a pair of florets (Figure 5A). In *Bif1* heterozygous plants, only 64% of spikelets produced two florets (Figure 5A), while in *Bif1* homozygotes only 3% of spikelets produced two florets (Figure 5A). These results indicate that in *Bif1* mutants, SMs are defective as they are unable to initiate the normal number of tertiary axillary meristems, FMs.

Normal tassels produce florets that contain a lemma, a palea, two lodicules, and three stamens. Quantitative analysis indicated that in *Bif1* mutants, the florets had fewer floral organs than normal with the homozygote being more severely affected than the heterozygote (Figure 5, B and C). The number of lemmas and paleae was reduced in *Bif1* mutants with 87% of spikelets from *Bif1* heterozygotes and 56% of spikelets from *Bif1* homozygotes producing both organs (Figure 5B). Lodicules were not counted as their small size and transparency made them difficult to count with accuracy under a dissecting microscope. Stamen number was reduced in *Bif1* mutants with only 29% of *Bif1/+* florets and 12% of *Bif1/Bif1* florets containing the normal three stamens (Figure 5C). Interestingly, a small percentage of *Bif1* mutant florets contained four stamens, indicating that floral organ number could be increased as well as decreased. The failure to initiate the normal number of floral organs indicates that FMs are also defective in *Bif1* mutants.

Expression studies show that *bif2* and *ba1* are expressed at a lower level in *Bif1* mutants: Like *Bif1*, *bif2* and *ba1* mutants are also defective in the initiation of all types of axillary meristems in the inflorescence (McSteen and Hake 2001; Ritter *et al.* 2002). To determine whether the *Bif1* mutation affected the expression of *bif2* or *ba1*, real-time RT–PCR experiments were performed. *bif2* and *ba1* are both expressed in tassels and ears in normal plants (Gallavotti *et al.* 2004; McSteen *et al.* 2007). *bif2* is expressed in axillary meristems, lateral organs, and vasculature while *ba1* has a more restricted expression pattern during axillary meristem initiation (Gallavotti *et al.* 2004; McSteen *et al.* 2007). RNA was isolated from immature tassels and ears of plants homozygous for *Bif1* and from normal siblings.

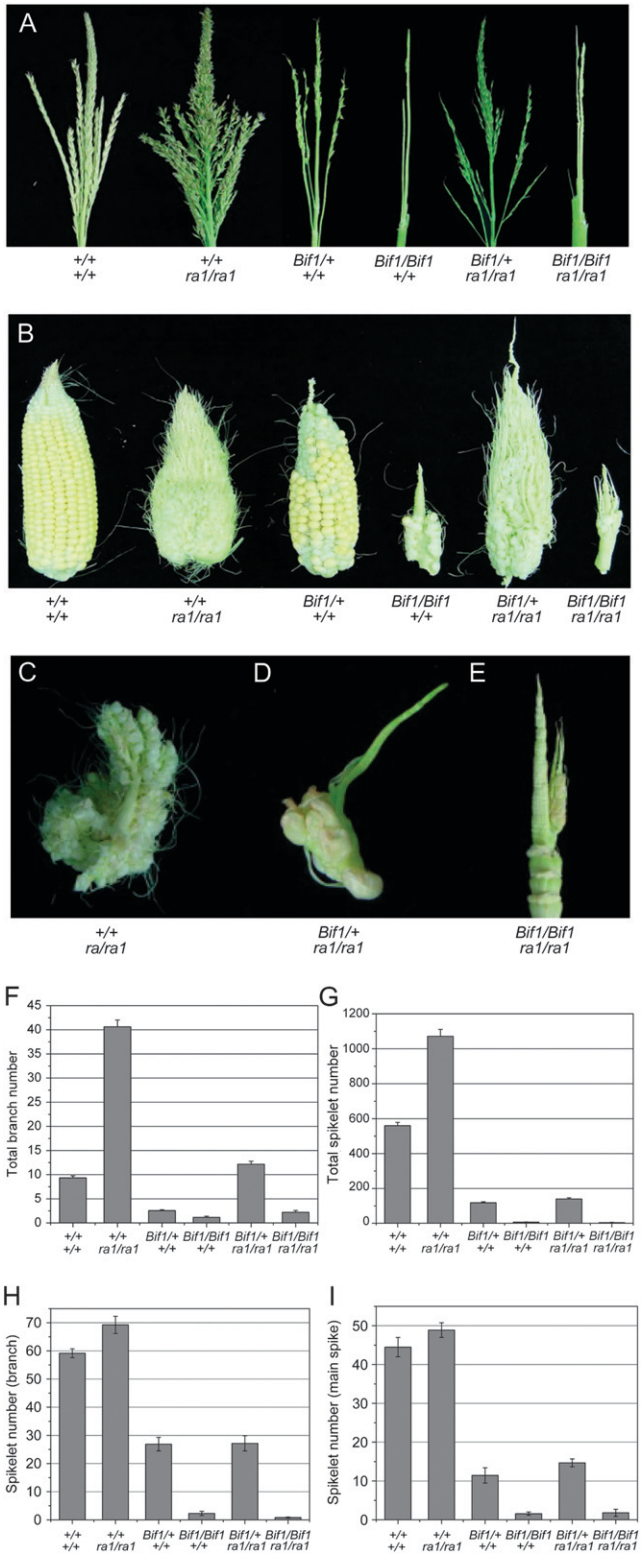

FIGURE 4.—Analysis of *Bif1; ra1* double mutants. (A) Mature tassel phenotype showing all genetic classes from a segregating *Bif1*; *ra1* family. (B) Ear phenotype of a segregating *Bif1; ra1* family. (C–E) Higher-magnification images showing individual branches from ears. (C) Branch from a *ra1/ra1* ear. (D) Branch from a *Bif1/+; ra1/ra1* ear. (E) *Bif1/Bif1; ra1/ra1* ear. (F–I) Quantitative analysis of *Bif1; ra1* double mutants. For all charts, bars represent mean value of the data set, and error bars represent standard error of the mean.

Real-time RT–PCR experiments indicated that both *bif2* and *ba1* RNA levels were reduced in tassels and ears of plants homozygous for *Bif1* (Figure 6, A–D). *bif2* levels were reduced to 36–62% of normal levels in tassel and ears, respectively (Figure 6, A and B), some of which could be explained by the reduction in the number of BMs, SPMs, SMs, FMs, and floral organs in *Bif1* mutants. On the other hand, *ba1* levels were dramatically reduced to 4–13% of normal levels (Figure 6, C and D). Considering that *ba1* is expressed in a very restricted pattern as axillary meristems initiate, these results provide further support that the *Bif1* mutation affects early stages of axillary meristem initiation.

Double-mutant analysis indicates that *bif1* and *bif2* play a role in vegetative development: *bif2* mutants have a phenotype very similar to that of *Bif1* homozygotes, with very few tassel branches and spikelets (McSteen and Hake 2001; McSteen *et al.* 2007). To determine the genetic interaction between *Bif1* and *bif2*, double-mutant lines were constructed. *Bif1; bif2* double-mutant plants had very dramatic effects on both vegetative and inflorescence development.

Inflorescence phenotype: The inflorescence phenotype of *Bif1; bif2* double mutants was more severe than that of either single mutant with no branches or spikelets (Figure 7, A–C). Quantitative analysis showed that the absence of spikelets in *Bif1/Bif1; bif2/bif2* double mutants was a statistically significant reduction in spikelet number compared to *Bif1/Bif1* (*P*-value = 0.004) or *bif2* single mutants (*P*-value = 0.001, Figure 7C). Furthermore, genetic and molecular analyses indicated that plants that were heterozygous for *Bif1* and homozygous for *bif2* resembled *Bif1* homozygotes (Figure 7, A–C). These results suggest that *bif1* and *bif2* play redundant roles in branch and spikelet initiation in the inflorescence.

Vegetative phenotype: Bif1; bif2 double-mutant plants were less than half the height of normal plants (Figure 7, D and E). To determine if the reduction in plant height was due to a difference in the number of phytomers produced, the number of leaves were counted (Figure 7F). Both *Bif1* and *bif2* (McSteen *et al.* 2007) have a minor effect on leaf number on their own, with a small but statistically significant reduction in the number of leaves compared to normal siblings (*P*-value = 0.001, Figure 7F). However, the *Bif1/Bif1; bif2/bif2* double mutant had a nonadditive effect with a large and significant reduction in leaf number compared to either *Bif1/Bif1* (*P*-value <0.001) or *bif2/bif2* (*P*-value = 0.001) single

(F) Average number of branches per tassel. (G) Average number of spikelets per tassel. (H) Average number of spikelets per branch, measured on a branch at the base of the tassel. (I) Average number of spikelets in the top 2 cm of the tassel main spike.

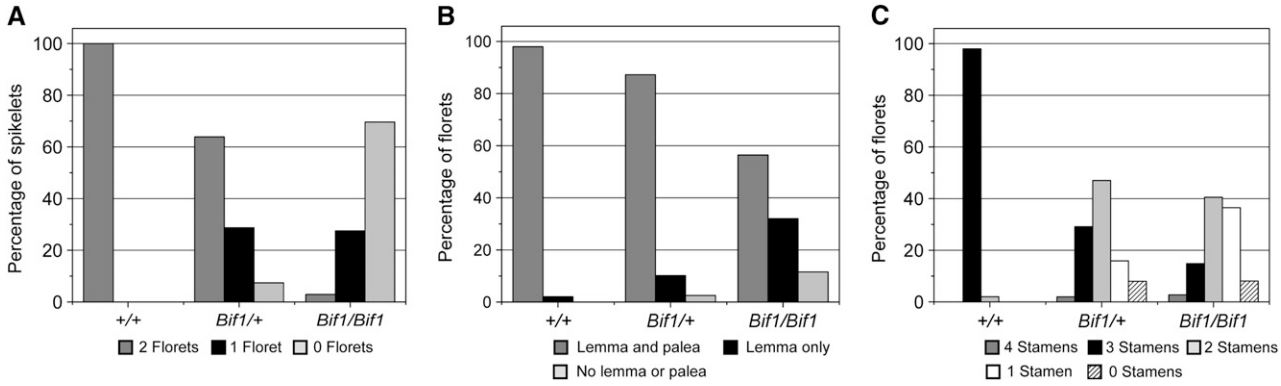

FIGURE 5.—Quantification of floret and floral organ numbers in *Bif1* mutants. (A) Percentage of spikelets containing two, one, or zero florets per spikelet. (B) Quantification of lemma and palea number per floret. (C) Percentage of florets containing the indicated number of stamens per floret.

mutants. The dramatic effect on leaf number in the *Bif1; bif2* double mutant implies that *bif1* and *bif2* also play redundant roles in the production of leaves by the vegetative shoot apical meristem.

Double-mutant analysis indicates that *Bif1* is epistatic to *ba1* in the tassel: The *barren stalk1* (*ba1*) mutant is deficient in both vegetative and inflorescence axillary meristem initiation and as a result lacks tillers and ears, as well as branches and spikelets in the tassel (RITTER *et al.* 2002; GALLAVOTTI *et al.* 2004). Although epistasis is challenging to determine when mutants have a similar phenotype, *Bif1* mutants can be distinguished from *ba1* mutants by the appearance of the inflorescence stem (rachis). *Bif1* mutants have a smooth thin rachis, while *ba1* mutants have a thick rachis with very regular pronounced protrusions due to the production of larger than normal suppressed bract primordia (RITTER *et al.* 2002). *Bif1/+; ba1/ba1* double mutants resembled *ba1* single mutants; however, the surface of the rachis was slightly smoother than usually observed in *ba1* tassels (Figure 8A). *Bif1/Bif1; ba1/ba1* double mutants resembled *Bif1* homozygotes with a smooth thin tassel rachis. As the *Bif1/Bif1; ba1/ba1* double mutant abolished the regular protrusions normally seen in *ba1* mutants, this indicates that *Bif1* is epistatic to *ba1* in the tassel. The inflorescence phenotype of the double mutant was not enhanced with respect to spikelet number, which was not unexpected as *ba1* mutants typically do not produce any spikelets (Figure 8B). Similarly, the double mutant did not produce any ears (Figure 8C). Moreover, this analysis also showed that the *Bif1* mutants alone did not have any defects in the production of ears

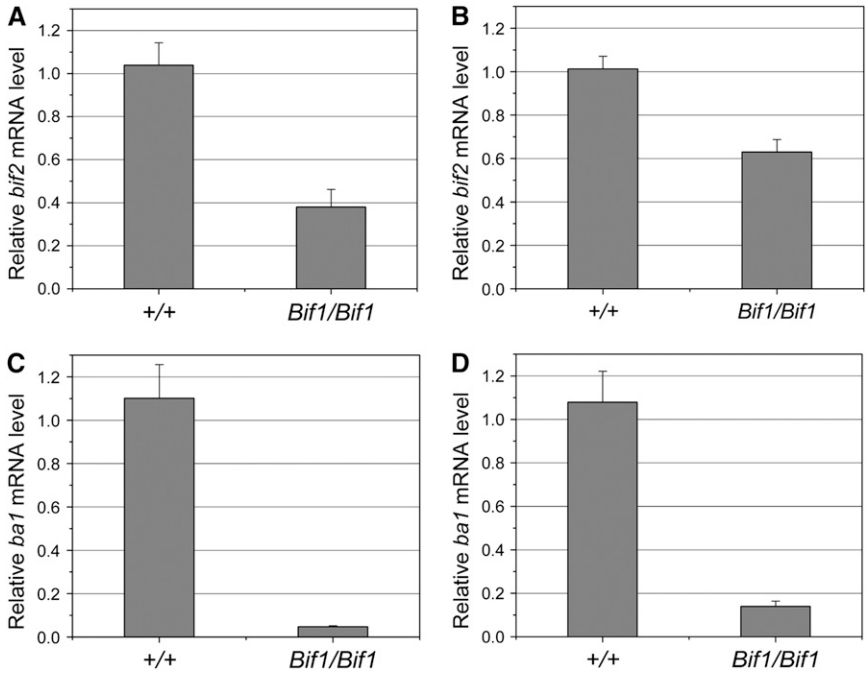

FIGURE 6.—Real-time RT–PCR analysis of the expression of *bif2* and *ba1* in *Bif1* mutants. (A) Expression level of *bif2* in the immature tassel of *Bif1* mutants relative to normal siblings. (B) Expression level of *bif2* in the immature ears of *Bif1* mutants relative to normal siblings. (C) Expression level of *ba1* in the immature tassel of *Bif1* mutants relative to normal siblings. (D) Expression level of *ba1* in the immature ears of *Bif1* mutants relative to normal siblings. Mean plus or minus SE is shown for one representative experiment using three biological and three technical replicates for each sample.

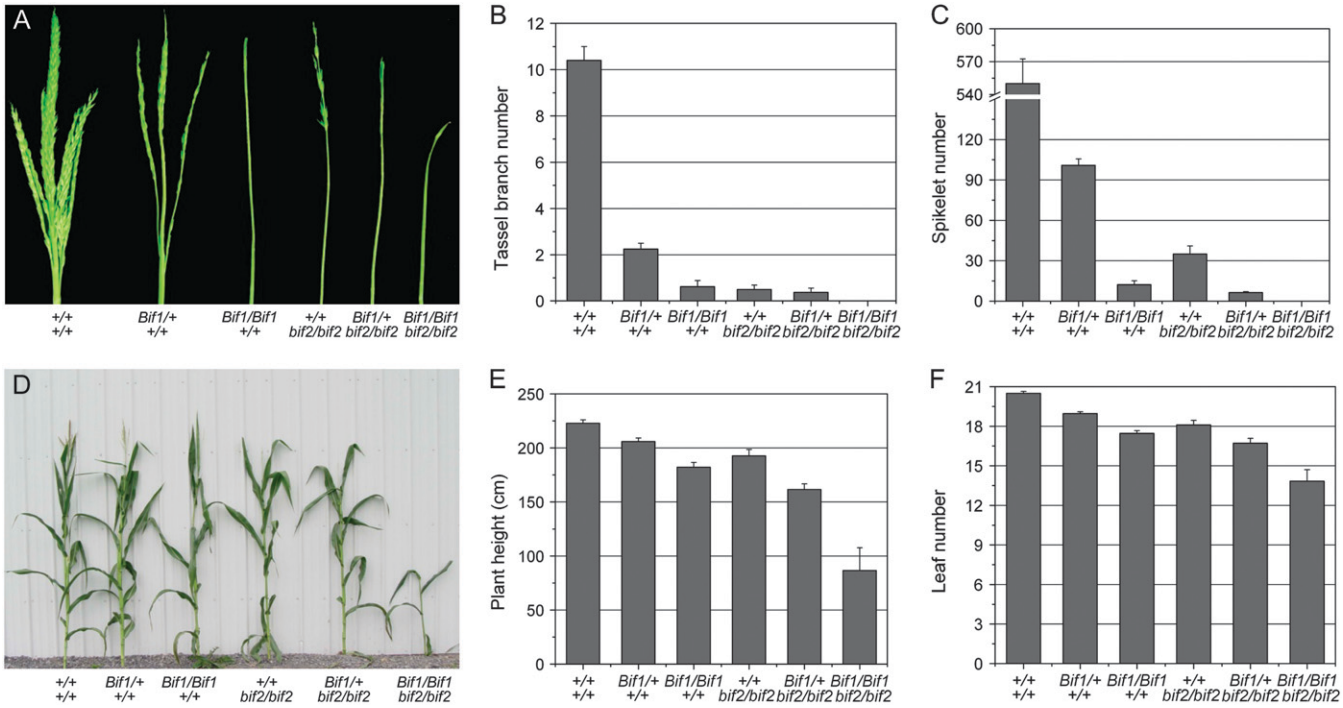

FIGURE 7.—Analysis of *Bif1; bif2* double mutants. (A) Mature tassel phenotype of a *Bif1; bif2* segregating family. (B and C) Quantification of tassel characteristics in a *Bif1*; *bif2* segregating family. (B) Average tassel branch number. (C) Average spikelet number per tassel. (D) Vegetative phenotype of a *Bif1; bif2* family showing reduced plant height in *Bif1; bif2* double mutants. (E and F) Quantification of vegetative phenotypes. (E) Average plant height in centimeters. (F) Average leaf number.

(Figure 8C). Unlike the interaction between *Bif1* and *bif2*, there was no enhancement of the vegetative defects of *Bif1* by *ba1* (data not shown), indicating that *ba1* does not play a redundant role in leaf initiation during vegetative development.

***Bif1* mutants have a reduced level of auxin transport:** As *Bif1* mutants had such a dramatic interaction with *bif2*, which plays a role in auxin transport, we tested whether *Bif1* mutants also have defects in auxin transport. *bif2* mutants have a reduced level of auxin transport in the mature inflorescence stem of the tassel (McSTEEN *et al.* 2007). Preliminary experiments showed that *Bif1* mutants similarly had reduced transport in the mature tassel inflorescence stem (data not shown). However, both *Bif1* and *bif2* mutants have reduced vasculature in the mature inflorescence stem (McSTEEN *et al.* 2007 and data not shown). *Bif1* mutants also have a reduction in vasculature in the immature tassel inflorescence early in development (supplemental Figure S1, A–C). However, *Bif1* mutants do not have significant reduction in vasculature in the developing ear inflorescence (supplemental Figure S1, D–F). Therefore, to determine if *Bif1* mutants had defects in auxin transport early in development, we developed a protocol to measure auxin transport within the ear inflorescence.

Immature ear inflorescences up to 2 cm in length were incubated overnight in either orientation in a solution of 1.5 μM ^{3}H-labeled IAA. Wild-type ears showed an appreciable level of basipetal transport that was inhibited by co-incubation with 20 μM *N*-1-naphthylphthalamic acid (NPA), a frequently used auxin transport inhibitor (Figure 9A, lanes 1 and 2). However, acropetal transport was very low at this point in development (Figure 9A, lanes 3 and 4).

To test whether *Bif1* ear inflorescences had a reduced level of auxin transport, basipetal transport was measured in plants that were heterozygous or homozygous for *Bif1* compared to normal siblings (Figure 9B). Plants that were heterozygous for *Bif1* had approximately one-third the level of transport as normal siblings (Figure 9B, lane 3), and these levels were further reduced by co-incubation with 20 μM NPA (Figure 9B, lane 4). Homozygous *Bif1* ears had an ever further reduction in active auxin transport (Figure 9B, lane 5), which was not significantly different from that of normal siblings treated with NPA (P-value = 0.75). Therefore, *Bif1* mutants have a reduced level of auxin transport, indicating that the primary defect in *Bif1* mutants may be in the regulation of auxin transport.

DISCUSSION

We have identified a new player in the pathway for axillary meristem initiation during maize inflorescence development. *Bif1* mutants have a very similar phenotype to *bif2* mutants with defects in the initiation of all axillary meristems in the inflorescence. The synergistic interaction of *Bif1* with *bif2* indicates that *bif1* acts

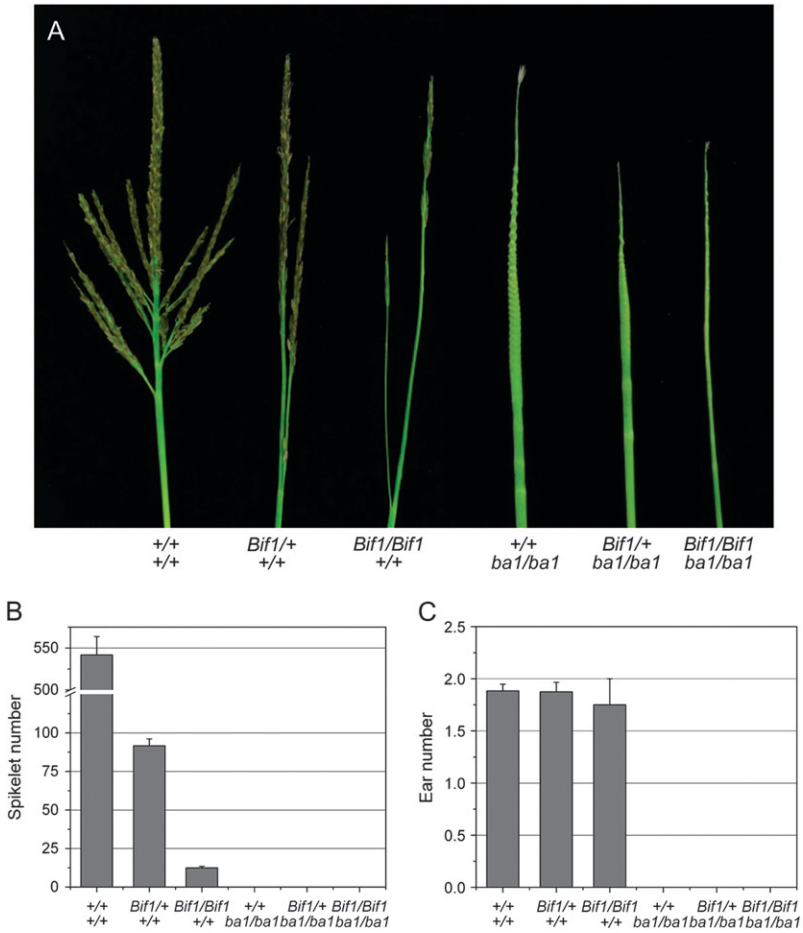

FIGURE 8.—Analysis of *Bif1; ba1* double mutants. (A) Mature tassel phenotype of *Bif1; ba1* family. (B) Average number of spikelets per tassel. (C) Average number of ears per plant.

redundantly with *bif2* during both vegetative and inflorescence development. We propose that the defects in *Bif1* mutants are caused by a reduction in auxin transport and that the function of *bif1* is to regulate auxin transport.

***bif1* plays a role in axillary meristem initiation:** Plants that are homozygous for *Bif1* have a very similar phenotype to *bif2* mutants (McSteen and Hake 2001).

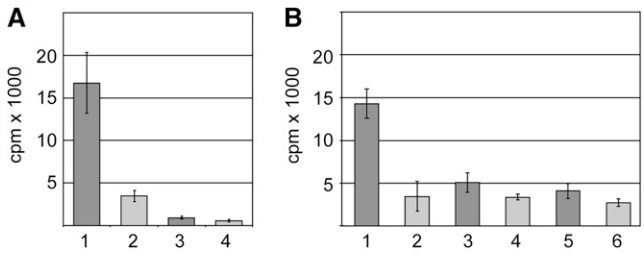

FIGURE 9.—Measurement of auxin transport in normal and *Bif1* inflorescences. Dark shading, without NPA; light shading, with NPA. (A) Measurement of basipetal (lanes 1 and 2) and acropetal (lanes 3 and 4) transport in normal ears. (B) Measurement of basipetal transport in immature ears of a family segregating for *Bif1*. Lanes 1 and 2, normal siblings; lanes 3 and 4, *Bif1*/+; lanes 5 and 6, *Bif1/Bif1*.

Similarities with *bif2* mutants include a reduction in the number of branches, spikelets, florets, and floral organs in the tassel and a reduction in kernel number in the ear. Moreover, *Bif1* mutants produce single instead of paired spikelets, which is also characteristic of *bif2* mutants. The tassel and ear rachis is smooth with occasional irregular ridges, similar to *bif2*. In addition, the apical ear inflorescence meristem can be fasciated, similar to *bif2*.

Characterization of the developing inflorescence by SEM analysis, histology, and *kn1* expression shows that there is a specific defect in axillary meristem initiation in *Bif1* mutants. We propose that *bif1* plays a role in axillary meristem initiation in the inflorescence. All axillary meristems in the inflorescence—BM, SPM, SM, and FM—are affected in the mutants. However, unlike *bif2*, *Bif1* mutants do not have defects in the initiation of the axillary meristem that gives rise to the ear shoot. Ears are produced in *Bif1* mutants as normal and there is no enhancement of the ear number defects in *Bif1; bif2* double mutants (data not shown). Moreover, unlike *bif2*, double-mutant analysis with *teosinte branched1* (*tb1*) (Doebley *et al.* 1997; Hubbard *et al.* 2002; McSteen *et al.* 2007) shows that the *Bif1* mutation does not have a major effect on vegetative axillary meristem (tiller) pro-

duction (data not shown). Therefore, one of the few differences between *Bif1* and *bif2* mutations is the extent of their effect on tiller and ear production.

During vegetative development, *Bif1* mutants have a small but significant reduction in the number of leaves, resulting in a concomitant reduction in plant height. *bif2* mutants also have a minor effect on the initiation of leaves during vegetative development (McSteen *et al.* 2007). The dramatic effect of the *Bif1; bif2* double mutant on vegetative development indicates that *bif1* and *bif2* play redundant roles in the production of leaves by the vegetative apical meristem. Therefore, our analysis shows that in addition to the role of *bif1* and *bif2* in initiation of axillary meristems during inflorescence development, *bif1* and *bif2* also play overlapping roles in the production of lateral organs during vegetative development.

Role of *bif1* in auxin transport: Gradients of auxin are required for polar growth in plants (Benkova *et al.* 2003; Heisler *et al.* 2005). In *pinformed1* (*pin1*) and *pinoid* (*pid*) mutants in Arabidopsis, a reduction in auxin transport abolishes the initiation of axillary meristems, leading to a "*pin*" inflorescence phenotype analogous to the *barren inflorescence* phenotype in maize (Okada *et al.* 1991; Bennett *et al.* 1995; Galweiler *et al.* 1998; Reinhardt *et al.* 2003). Double mutants in members of the *YUCCA* gene family, required for auxin biosynthesis, also cause a *pin* inflorescence phenotype (Cheng *et al.* 2006). However, either loss or gain of function of the transcription factor *MONOPTEROS* leads to a *pin* inflorescence phenotype, illustrating that loss or gain of auxin signaling abolishes axillary meristem initiation (Przemeck *et al.* 1996; Hardtke *et al.* 2004). Therefore, defects in auxin biosynthesis, transport, or response lead to a failure to initiate axillary meristems in the inflorescence in Arabidopsis (Cheng and Zhao 2007).

We propose that *bif1* acts together with *bif2* in the control of auxin transport in the maize inflorescence. Many of the phenotypes seen in *Bif1* and *bif2* mutants are also seen in plants treated with auxin transport inhibitors (Wu and McSteen 2007). For example, the failure to initiate axillary meristems in the inflorescence, single spikelets, reduced vasculature, and fewer leaves are also seen in plants that have been treated with polar auxin transport inhibitors (Scanlon 2003; Wu and McSteen 2007). Therefore, we tested the levels of auxin transport in the inflorescence of *Bif1* mutants and found auxin transport to be reduced, implying that *bif1* plays a role in auxin transport.

The *Bif1* mutation is semidominant so it could be either a dominant loss-of-function (*e.g.*, antimorph or hypomorph) or a dominant gain-of-function (*e.g.*, hypermorph or neomorph) mutation. It was not possible to use dosage analysis to determine whether *Bif1* is a loss- or gain-of-function mutation as *Bif1* is not uncovered by the known translocation lines on chromosome 8. However, as the *Bif1* mutation causes a reduction of auxin transport, we can conclude that the *bif1* gene is either a positive or a negative regulator of auxin transport.

Genetic interaction between *Bif1* and other *barren inflorescence* mutations: To determine the genetic interaction between *Bif1* and previously known *barren inflorescence* mutations we performed double-mutant and expression analyses. We infer that *bif1* acts upstream of *ba1* as the *Bif1; ba1* double mutant resembled *Bif1* in the tassel. In addition, the levels of *ba1* expression were dramatically reduced in *Bif1* mutants. Further support for this hypothesis is provided by the proposal that *ba1* acts downstream of auxin transport (Wu and McSteen 2007). The *ba1* mutant produces bracts in a very regular pattern, indicating that phyllotaxis is not disrupted in the mutant and that auxin transport is normal (Ritter *et al.* 2002). Furthermore, *ba1* is not expressed after treatment with auxin transport inhibitors, indicating that *ba1* expression depends on auxin transport (Wu and McSteen 2007). We propose that *ba1*, being a transcription factor, is required for the response to the auxin signal for axillary meristem initiation. We propose that *bif1* acts upstream of auxin transport and hence is upstream of *ba1*.

Expression analysis shows that *bif2* levels are somewhat reduced in *Bif1* mutants. Some of the reduction in *bif2* expression could be explained by the absence of structures that express *bif2*, or this result could imply that *Bif1* acts upstream of *bif2*. However, the synergistic effect observed in *Bif1; bif2* double mutants implies that *bif1* and *bif2* have overlapping functions. Both mutants have a very similar phenotype but the double mutant is much more severe than either single mutant, indicating that *bif1* and *bif2* may play redundant roles in vegetative and inflorescence development. The dosage effect of the *Bif1; bif2* interaction further supports that they affect the same process. From the results of the double-mutant and expression analyses, together with previous results, we propose that *bif1* and *bif2* both act upstream of auxin transport.

To determine the molecular mechanism by which *bif1* regulates auxin transport, future work will identify the *bif1* gene by map-based cloning. With the sequencing of the maize genome and the availability of the genome sequence of related grasses, chromosome walking is now routine in maize (Salvi *et al.* 2002; Wang *et al.* 2005; Alleman *et al.* 2006; Bortiri *et al.* 2006a,b; Satoh-Nagasawa *et al.* 2006; Taramino *et al.* 2007). Many regulators of auxin transport have been identified in other species; however, only *pin* and *pid* mutants have a *pin* inflorescence phenotype (Brown *et al.* 2001; Gil *et al.* 2001; Noh *et al.* 2001; Geisler *et al.* 2003; Geldner *et al.* 2003; Multani *et al.* 2003; Bennett *et al.* 2006; Sieburth *et al.* 2006). The closest maize homologs of *pin* and *pid* do not map to *Bif1*, indicating that the *bif1* gene possibly may be a novel regulator of auxin transport in the inflorescence.

P.M. thanks Sarah Hake for her mentorship early in the development of the *barren inflorescence* project. We thank Tony Omeis, W. Scott Harkcom, and Bob Oberheim for plant care in the Department of Biology greenhouse and in the Departments of Horticulture and Crop and Soil Sciences farm sites in Rock Springs, Pennsylvania. We thank Carrie Barrios for performing some of the genetic crosses, Molly Saweikis for initial SEM analysis, Missy Hazen for training on the SEM, Deb Grove for assistance with real-time RT–PCR experiments, and undergraduate students Jason Hoar, Jeffrey Buterbaugh, Kim Phillips, Matt Davis, and Chris Cook for assistance with analysis of double mutants in the field. We thank members of the Braun and McSteen labs for discussion and critical reading of the manuscript. This research was funded by the Huck Institutes of Life Science graduate fellowship to S.B. and by National Science Foundation grant no. IOS-0416616 to P.M.

LITERATURE CITED

Alleman, M., L. Sidorenko, K. McGinnis, V. Seshadri, J. E. Dorweiler *et al.*, 2006 An RNA-dependent RNA polymerase is required for paramutation in maize. Nature **442:** 295–298.

Benjamins, R., A. Quint, D. Weijers, P. Hooykaas and R. Offringa, 2001 The PINOID protein kinase regulates organ development in Arabidopsis by enhancing polar auxin transport. Development **128:** 4057–4067.

Benkova, E., M. Michniewicz, M. Sauer, T. Teichmann, D. Seifertova *et al.*, 2003 Local, efflux-dependent auxin gradients as a common module for plant organ formation. Cell **115:** 591–602.

Bennett, S. R. M., J. Alvarez, G. Bossinger and D. R. Smyth, 1995 Morphogenesis in *pinoid* mutants of *Arabidopsis thaliana*. Plant J. **8:** 505–520.

Bennett, T., T. Sieberer, B. Willett, J. Booker, C. Luschnig *et al.*, 2006 The Arabidopsis MAX pathway controls shoot branching by regulating auxin transport. Curr. Biol. **16:** 553–563.

Bommert, P., N. Satoh-Nagasawa, D. Jackson and H. Y. Hirano, 2005 Genetics and evolution of inflorescence and flower development in grasses. Plant Cell Physiol. **46:** 69–78.

Bortiri, E., and S. Hake, 2007 Flowering and determinacy in maize. J. Exp. Bot. **58:** 909–916.

Bortiri, E., G. Chuck, E. Vollbrecht, T. Rocheford, R. Martienssen *et al.*, 2006a *ramosa2* encodes a LATERAL ORGAN BOUNDARY domain protein that determines the fate of stem cells in branch meristems of maize. Plant Cell **18:** 574–585.

Bortiri, E., D. Jackson and S. Hake, 2006b Advances in maize genomics: the emergence of positional cloning. Curr. Opin. Plant Biol. **9:** 164–171.

Brown, D. E., A. M. Rashotte, A. S. Murphy, J. Normanly, B. W. Tague *et al.*, 2001 Flavonoids act as negative regulators of auxin transport in vivo in *Arabidopsis*. Plant Physiol. **126:** 524–535.

Chen, J., and S. L. Dellaporta, 1994 Urea based plant DNA miniprep, pp. 526–527 in *The Maize Handbook*, edited by M. Freeling and V. Walbot. Springer-Verlag, New York.

Cheng, P. C., R. I. Greyson and D. B. Walden, 1983 Organ initiation and the development of unisexual flowers in the tassel and ear of *Zea mays*. Am. J. Bot. **70:** 450–462.

Cheng, Y., X. Dai and Y. Zhao, 2007 Auxin synthesized by the YUCCA flavin monooxygenases is essential for embryogenesis and leaf formation in Arabidopsis. Plant Cell **19:** 2430–2439.

Cheng, Y. F., and Y. D. Zhao, 2007 A role for auxin in flower development. J. Integr. Plant Biol. **49:** 99–104.

Cheng, Y. F., X. H. Dai and Y. D. Zhao, 2006 Auxin biosynthesis by the YUCCA flavin monooxygenases controls the formation of floral organs and vascular tissues in Arabidopsis. Genes Dev. **20:** 1790–1799.

Christensen, S. K., N. Dagenais, J. Chory and D. Weigel, 2000 Regulation of auxin response by the protein kinase PINOID. Cell **100:** 469–478.

Clifford, H. T., 1987 Spikelet and floral morphology, pp. 21–30 in *Grass Systematics and Evolution*, edited by T. R. Soderstrom, K. W. Hilu, C. S. Campbell and M. E. Barkworth. Smithsonion Institution Press, Washington, DC.

Coe, E. H., M. G. Neuffer and D. A. Hoisington, 1988 The genetics of corn, pp. 81–258 in *Corn and Corn Improvement*, edited by G. F. Sprague and J. W. Dudley. ASA-CSSA-SSSA, Madison, WI.

Doebley, J., A. Stec and L. Hubbard, 1997 The evolution of apical dominance in maize. Nature **386:** 485–488.

Gallavotti, A., Q. Zhao, J. Kyozuka, R. B. Meeley, M. Ritter *et al.*, 2004 The role of *barren stalk1* in the architecture of maize. Nature **432:** 630–635.

Galweiler, L., C. H. Guan, A. Muller, E. Wisman, K. Mendgen *et al.*, 1998 Regulation of polar auxin transport by AtPIN1 in Arabidopsis vascular tissue. Science **282:** 2226–2230.

Geisler, M., H. U. Kolukisaoglu, R. Bouchard, K. Billion, J. Berger *et al.*, 2003 TWISTED DWARF1, a unique plasma membrane-anchored immunophilin-like protein, interacts with Arabidopsis multidrug resistance-like transporters AtPGP1 and AtPGP19. Mol. Biol. Cell **14:** 4238–4249.

Geldner, N., N. Anders, H. Wolters, J. Keicher, W. Kornberger *et al.*, 2003 The Arabidopsis GNOM ARF-GEF mediates endosomal recycling, auxin transport, and auxin-dependent plant growth. Cell **112:** 219–230.

Gernart, W., 1912 A new subspecies of *Zea mays* L. Am. Nat. **46:** 616–622.

Gil, P., E. Dewey, J. Friml, Y. Zhao, K. C. Snowden *et al.*, 2001 BIG: a calossin-like protein required for polar auxin transport in Arabidopsis. Genes Dev. **15:** 1985–1997.

Hardtke, C. S., W. Ckurshumova, D. P. Vidaurre, S. A. Singh, G. Stamatiou *et al.*, 2004 Overlapping and non-redundant functions of the Arabidopsis auxin response factors MONOPTEROS and NONPHOTOTROPIC HYPOCOTYL 4. Development **131:** 1089–1100.

Heisler, M. G., C. Ohno, P. Das, P. Sieber, G. V. Reddy *et al.*, 2005 Patterns of auxin transport and gene expression during primordium development revealed by live imaging of the Arabidopsis inflorescence meristem. Curr. Biol. **15:** 1899–1911.

Hubbard, L., P. McSteen, J. Doebley and S. Hake, 2002 Expression patterns and mutant phenotype of *teosinte branched1* correlate with growth suppression in maize and teosinte. Genetics **162:** 1927–1935.

Irish, E. E., 1996 Regulation of sex determination in maize. BioEssays **18:** 363–369.

Irish, E. E., 1997 Class II *tassel seed* mutations provide evidence for multiple types of inflorescence meristems in maize (Poaceae). Am. J. Bot. **84:** 1502–1515.

Jackson, D., B. Veit and S. Hake, 1994 Expression of maize *knotted1* related homeobox genes in the shoot apical meristem predicts patterns of morphogenesis in the vegetative shoot. Development **120:** 405–413.

Kellogg, E. A., 2000 The grasses: a case study in macroevolution. Annu. Rev. Ecol. Syst. **31:** 217–238.

Kellogg, E. A., 2007 Floral displays: genetic control of grass inflorescences. Curr. Opin. Plant Biol. **10:** 26–31.

Kerstetter, R. A., D. Laudencia-Chingcuanco, L. G. Smith and S. Hake, 1997 Loss-of-function mutations in the maize homeobox gene, *knotted1*, are defective in shoot meristem maintenance. Development **124:** 3045–3054.

Lee, S. H., and H. T. Cho, 2006 PINOID positively regulates auxin efflux in Arabidopsis root hair cells and tobacco cells. Plant Cell **18:** 1604–1616.

Livak, K. J., and T. D. Schmittgen, 2001 Analysis of relative gene expression data using real-time quantitative PCR and the $2^{-\Delta\Delta C}_{T}$ method. Methods **25:** 402–408.

McSteen, P., 2006 Branching out: the *ramosa* pathway and the evolution of grass inflorescence morphology. Plant Cell **18:** 518–522.

McSteen, P., and S. Hake, 1998 Genetic control of plant development. Curr. Opin. Biotechnol. **9:** 189–195.

McSteen, P., and S. Hake, 2001 *barren inflorescence2* regulates axillary meristem development in the maize inflorescence. Development **128:** 2881–2891.

McSteen, P., and O. Leyser, 2005 Shoot branching. Annu. Rev. Plant Biol. **56:** 353–374.

McSteen, P., D. Laudencia-Chingcuanco and J. Colasanti, 2000 A floret by any other name: control of meristem identity in maize. Trends Plant Sci. **5:** 61–66.

McSteen, P., S. Malcomber, A. Skirpan, C. Lunde, X. Wu *et al.*, 2007 *barren inflorescence2* encodes a co-ortholog of the *PINOID* serine/threonine kinase and is required for organogenesis dur-

ing inflorescence and vegetative development in maize. Plant Physiol. **144:** 1000–1011.

Multani, D. S., S. P. Briggs, M. A. Chamberlin, J. J. Blakeslee, A. S. Murphy *et al.*, 2003 Loss of an MDR transporter in compact stalks of maize *br2* and sorghum *dw3* mutants. Science **302:** 81–84.

Neuffer, M. G., and K. A. Sheridan, 1977 Dominant mutants from EMS treated pollen. Maize Newsl. **51:** 59–60.

Neuffer, M. G., E. H. Coe and S. R. Wessler, 1997 *The Mutants of Maize*. Cold Spring Harbor Laboratory Press, Plainview, NY.

Noh, B., A. S. Murphy and E. P. Spalding, 2001 Multidrug resistance-like genes of Arabidopsis required for auxin transport and auxin-mediated development. Plant Cell **13:** 2441–2454.

Okada, K., J. Ueda, M. K. Komaki, C. J. Bell and Y. Shimura, 1991 Requirement of the auxin polar transport system in early stages of Arabidopsis floral bud formation. Plant Cell **3:** 677–684.

Przemeck, G. K. H., J. Mattsson, C. S. Hardtke, Z. R. Sung and T. Berleth, 1996 Studies on the role of the Arabidopsis gene *MONOPTEROS* in vascular development and plant cell axialization. Planta **200:** 229–237.

Reinhardt, D., T. Mandel and C. Kuhlemeier, 2000 Auxin regulates the initiation and radial position of plant lateral organs. Plant Cell **12:** 507–518.

Reinhardt, D., E. R. Pesce, P. Stieger, T. Mandel, K. Baltensperger *et al.*, 2003 Regulation of phyllotaxis by polar auxin transport. Nature **426:** 255–260.

Ritter, M. K., C. M. Padilla and R. J. Schmidt, 2002 The maize mutant *barren stalk1* is defective in axillary meristem development. Am. J. Bot. **89:** 203–210.

Salvi, S., R. Tuberosa, E. Chiapparino, M. Maccaferri, S. Veillet *et al.*, 2002 Toward positional cloning of *Vgt1*, a QTL controlling the transition from the vegetative to the reproductive phase in maize. Plant Mol. Biol. **48:** 601–613.

Satoh-Nagasawa, N., N. Nagasawa, S. Malcomber, H. Sakai and D. Jackson, 2006 A trehalose metabolic enzyme controls inflorescence architecture in maize. Nature **441:** 227–230.

Scanlon, M. J., 2003 The polar auxin transport inhibitor N-1-naphthylphthalamic acid disrupts leaf initiation, KNOX protein regulation, and formation of leaf margins in maize. Plant Physiol. **133:** 597–605.

Sheridan, W. F., 1988 Maize developmental genetics: genes of morphogenesis. Annu. Rev. Genet. **22:** 353–385.

Sieburth, L. E., G. K. Muday, E. J. King, G. Benton, S. Kim *et al.*, 2006 SCARFACE encodes an ARF-GAP that is required for normal auxin efflux and vein patterning in Arabidopsis. Plant Cell **18:** 1396–1411.

Steeves, T., and I. Sussex, 1989 *Patterns in Plant Development*. Cambridge University Press, Cambridge, UK.

Taramino, G., M. Sauer, J. L. Stauffer, D. Multani, X. Niu *et al.*, 2007 The maize (*Zea mays* L.) *RTCS* gene encodes a LOB domain protein that is a key regulator of embryonic seminal and post-embryonic shoot-borne root initiation. Plant J. **50:** 649–659.

Veit, B., 2006 Stem cell signalling networks in plants. Plant Mol. Biol. **60:** 793–810.

Veit, B., R. J. Schmidt, S. Hake and M. F. Yanofsky, 1993 Maize floral development—new genes and old mutants. Plant Cell **5:** 1205–1215.

Vernoux, T., J. Kronenberger, O. Grandjean, P. Laufs and J. Traas, 2000 *PIN-FORMED 1* regulates cell fate at the periphery of the shoot apical meristem. Development **127:** 5157–5165.

Vollbrecht, E., L. Reiser and S. Hake, 2000 Shoot meristem size is dependent on inbred background and presence of the maize homeobox gene, *knotted1*. Development **127:** 3161–3172.

Vollbrecht, E., P. S. Springer, L. Goh, E. S. Buckler, IV and R. Martienssen, 2005 Architecture of floral branch systems in maize and related grasses. Nature **436:** 1119–1126.

Wang, H., T. Nussbaum-Wagler, B. Li, Q. Zhao, Y. Vigouroux *et al.*, 2005 The origin of the naked grains of maize. Nature **436:** 714–719.

Wu, X., and P. McSteen, 2007 The role of auxin transport during inflorescence development in maize, *Zea mays* (Poaceae). Am. J. Bot. **11:** 1745–1755.

Communicating editor: V. Sundaresan